

V-T Theory of Self Dynamic Response in a Monatomic Liquid

Giulia De Lorenzi-Venneri, Eric D. Chisolm, and Duane C. Wallace
Theoretical Division, Los Alamos National Laboratory, Los Alamos, New Mexico 87545
 (Dated: August 16, 2021)

A new theoretical model for self dynamic response is developed using Vibration-Transit (V-T) theory, and is applied to liquid sodium at all wavevectors q from the hydrodynamic regime to the free particle limit. In this theory the zeroth-order Hamiltonian describes the vibrational motion in a single random valley harmonically extended to infinity. This Hamiltonian is tractable, is evaluated *a priori* for monatomic liquids, and the same Hamiltonian (the same set of eigenvalues and eigenvectors) is used for equilibrium and nonequilibrium theory. Here, for the self intermediate scattering function $F^s(q, t)$, we find the vibrational contribution is in near perfect agreement with molecular dynamics (MD) through short and intermediate times, at all q . This is direct confirmation that normal mode vibrational correlations are present in the motion of the liquid state. The primary transit effect is diffusive motion of the vibrational equilibrium positions, as the liquid transits rapidly among random valleys. This motion is modeled as a standard random walk, and the resulting theoretical $F^s(q, t)$ is in excellent agreement with MD results at all q and t . In the limit $q \rightarrow \infty$, the theory automatically exhibits the correct approach to the free-particle limit. Also in the limit $q \rightarrow 0$, the hydrodynamic limit emerges as well. In contrast to the benchmark theories of generalized hydrodynamics and mode coupling, the present theory is near *a priori*, while achieving modestly better accuracy. Therefore, in our view, it constitutes an improvement over the traditional theories.

PACS numbers: 05.20.Jj, 63.50.+x, 61.20.Lc, 61.12.Bt

I. INTRODUCTION

Important advances have been made in the theory of equilibrium thermodynamic properties of liquids [1, 2]. These advances are characterized by the ability to calculate *a priori* the measured properties of real liquids, to an accuracy approaching the experimental accuracy itself [3, 4, 5]. The *a priori* nature of the theory is based on the key physical property of condensed matter, that the potential which governs the nuclear motion is given by electronic structure theory, in the form of the electronic groundstate energy as a function of the nuclear positions. In applying these broad theoretical foundations, two developments have been extremely helpful: (a) the development of pseudopotential perturbation theory which gives effective internuclear potentials for nearly-free-electron metals in crystal and liquid phases [6], and (b) the development of molecular dynamics (MD) computations to the point of providing highly accurate results, indeed capable of substituting for experimental data, when a good internuclear potential is used [7]. Based on these principles, *a priori* calculations have been made of binding energies of the elements [8], thermodynamic properties of crystals [9] and liquids [10], and liquid static structure factors [11, 12]. What is important for the present work, MD has proven its reliability for nonequilibrium properties, e.g. $S(q, \omega)$ for crystals [13] and liquids [7, 12, 14], liquid resistivity [15], and shear viscosity [16, 17].

V-T theory was introduced when it was found that a theory based on two components of the atomic motion can account for the equilibrium thermodynamic data of elemental liquids [18]: (a) normal-mode vibrations in one (any) random valley, providing $\gtrsim 90\%$ of the thermal energy and entropy, and (b) transits among a very large number of macroscopically equivalent random valleys, providing the remaining 10%. This theory is useful because the dominant vibrational motion is tractable, and its Hamiltonian can be evaluated for real liquids from electronic structure theory [19]. To test this theory beyond equilibrium properties, it was applied to dynamic response in liquid sodium, where the vibrational contribution alone was found to give an excellent account of experimental results for the Brillouin peak dispersion curve [20]. A small correction for transits then produced agreement with MD data for the entire $S(q, \omega)$ graphs [21]. At this point we could see the possibility of a liquid theory for both equilibrium and nonequilibrium properties based on the same dominant (vibrational) component of the motion. Such a theory could prove useful because traditional nonequilibrium theories primarily describe the decay of fluctuations, through processes encoded in e.g. friction coefficients and memory functions, and these are concepts not present in equilibrium theories. Our point is not that the traditional description is wrong, but that a good part of it is already contained in the same vibrational motion that underlies the equilibrium theory. This view motivates the present application of V-T theory to self dynamic response. This application will provide a serious test of our theory, since self dynamic response has been thoroughly analyzed by the traditional theories of generalized hydrodynamics [22] and mode coupling [23]. These analyses are discussed in liquid theory monographs, and have become a benchmark in dynamic response theories [24, 25].

The previous application of V-T theory to dynamic response was evaluated in the one-mode scattering approxima-

tion [21]. Here, to work at larger q , it is necessary to use the full vibrational theory, including normal-mode scattering in all orders, i.e. keeping the displacement autocorrelation functions in the exponent. This formulation has not been studied previously, and what it reveals is remarkable to say the least. The vibrational contribution alone, in *a priori* numerical evaluation at all q , is in near perfect agreement with MD calculations through short and intermediate times, and the vibrational contribution alone also converges to the correct theoretical free-particle behavior at large q . Then, accounting for transit motion in leading approximation produces a theory in excellent agreement with MD calculations at all q and t .

In Sec. IIA, the vibrational contribution to the self intermediate scattering function is derived, and its short-time behavior is examined, as well as its convergence to the free-particle limit. In Sec. IIB, the complete time dependence of the vibrational contribution is analyzed, and in Sec. IIC this contribution is compared with MD data. The transit induced correction to the vibrational contribution is derived and modeled in Sec. IID. The hydrodynamic limit is derived in Sec. IIE. The complete theoretical results, vibrational plus transit, are compared with MD in Sec. IIIA and the two-step process by which theory approaches the free-particle limit is analyzed in Sec. IIIB. The salient theoretical features are summarized and discussed in Secs. IVA and IVB, and V-T theory is compared and contrasted with the classic benchmark theories in Sec. IVC. A brief sketch of the operational procedure of V-T theory may be found in the Appendix.

II. THEORY

A. The Vibrational Contribution

We consider a system of N atoms in a cubic box at the density of the liquid, with periodic boundary conditions applied to the atomic motion. The atoms are labeled $K = 1, \dots, N$ and their positions are $\mathbf{r}_K(t)$ as functions of time t . The self component of the intermediate scattering function is [24, 25]

$$F^s(q, t) = \frac{1}{N} \left\langle \sum_K e^{-i\mathbf{q} \cdot (\mathbf{r}_K(t) - \mathbf{r}_K(0))} \right\rangle, \quad (1)$$

where the brackets indicate a motional average in an equilibrium state. The vibrational contribution expresses the motion in a single harmonic random valley extended to infinity [18]. In this motion each atom moves with displacement $\mathbf{u}_K(t)$ away from the fixed equilibrium position \mathbf{R}_K , so that

$$\mathbf{r}_K(t) = \mathbf{R}_K + \mathbf{u}_K(t). \quad (2)$$

Then the vibrational contribution to Eq. (1) becomes

$$F_{vib}^s(q, t) = \frac{1}{N} \left\langle \sum_K e^{-i\mathbf{q} \cdot (\mathbf{u}_K(t) - \mathbf{u}_K(0))} \right\rangle_{vib}, \quad (3)$$

where $\langle \dots \rangle_{vib}$ indicates an average over the vibrational motion in one (any) random valley. This is simplified by Bloch's theorem to

$$F_{vib}^s(q, t) = \frac{1}{N} \sum_K e^{-2W_K(\mathbf{q})} e^{\langle \mathbf{q} \cdot \mathbf{u}_K(t) \mathbf{q} \cdot \mathbf{u}_K(0) \rangle_{vib}}, \quad (4)$$

The displacement autocorrelation functions are expressed in terms of the normal vibrational modes λ [26]

$$\langle \mathbf{q} \cdot \mathbf{u}_K(t) \mathbf{q} \cdot \mathbf{u}_K(0) \rangle_{vib} = \frac{kT}{M} \sum_{\lambda} (\mathbf{q} \cdot \mathbf{w}_{K\lambda})^2 \frac{\cos \omega_{\lambda} t}{\omega_{\lambda}^2}, \quad (5)$$

where T is the temperature, M is the atomic mass, $\mathbf{w}_{K\lambda}$ is the Cartesian vector of the K component of eigenvector λ , and ω_{λ} is the corresponding frequency. The Debye-Waller factors are defined by

$$W_K(\mathbf{q}) = \frac{1}{2} \langle (\mathbf{q} \cdot \mathbf{u}_K(0))^2 \rangle_{vib}, \quad (6)$$

and are given by Eq. (5) evaluated at $t = 0$. In addition to the vibrational averages, the right sides of Eqs. (3) and (4) are to be averaged over the allowed \mathbf{q} -vectors at each q -magnitude, making $F_{vib}(q, t)$ a function only of q , as indicated.

Important properties of $F_{vib}^s(q, t)$ are determined by its short-time expansion. To find this behavior we write, from Eqs. (4)-(6),

$$\langle \mathbf{q} \cdot \mathbf{u}_K(t) \mathbf{q} \cdot \mathbf{u}_K(0) \rangle_{vib} - 2W_K(\mathbf{q}) = \frac{kT}{M} \sum_{\lambda} (\mathbf{q} \cdot \mathbf{w}_{K\lambda})^2 \frac{1}{\omega_{\lambda}^2} (\cos \omega_{\lambda} t - 1). \quad (7)$$

The expansion for $\omega_{\lambda} t \ll 1$ is

$$F_{vib}^s(q, t) = e^{-a(q)t^2} \frac{1}{N} \sum_K e^{b_K(\mathbf{q})t^4 - \dots}. \quad (8)$$

The value at $t = 0$ is

$$F_{vib}^s(q, 0) = 1, \quad (9)$$

which is the exact theoretical result, as can be seen from Eq. (1). The coefficient of t^2 is

$$a(q) = kTq^2/2M, \quad (10)$$

obtained with the aid of the eigenvector completeness relation [19]

$$\sum_{\lambda} w_{Ki,\lambda} w_{Lj,\lambda} = \delta_{KL} \delta_{ij}, \quad (11)$$

where i, j are the Cartesian directions. In studying the time dependence, it is advantageous to keep it in the exponent, as in Eq. (8), rather than to expand the exponential. The leading factor in Eq. (8) is the free-particle result, defined by

$$F_{free}^s(q, t) = e^{-a(q)t^2}. \quad (12)$$

Finally, the coefficients of t^4 in Eq. (8) are

$$b_K(\mathbf{q}) = \frac{kTq^2}{24M} \sum_{\lambda} (\hat{\mathbf{q}} \cdot \mathbf{w}_{K\lambda})^2 \omega_{\lambda}^2, \quad (13)$$

where the unit vector $\hat{\mathbf{q}}$ has been introduced so as to factor out q^2 . Without approximation, the K -dependence of the $b_K(\mathbf{q})$ cannot be ignored.

In dynamic response, free-particle motion becomes dominant at short times and distances. Free-particle behavior is contained in the self dynamic response [24, 25], and should emerge in the large- q limit of Eq. (4). Since the right side of Eq. (7) is negative and proportional to q^2 , as q increases $F_{vib}^s(q, t)$ will drop off more rapidly with increasing t . Therefore at high q only the lowest-order term in Eq. (7) will be relevant, so that

$$\lim_{q \rightarrow \infty} F_{vib}^s(q, t) = F_{free}^s(q, t). \quad (14)$$

The process of the approach to this limit will be examined below.

B. Free, Intermediate, and Convergence Periods

We calculated $F_{vib}^s(q, t)$ for the 17 q values listed in Table I. Representative graphs are shown in Fig. 1. Each curve has the same characteristic shape: it starts at 1, decreases on a uniform (q -independent) timescale, then levels off and converges to its long-time limit. The displacement autocorrelation functions, Eq. (5), decay to zero as time increases. This decay is called the ‘‘natural’’ decorrelation, and is responsible for the entire time dependence of $F_{vib}^s(q, t)$. Analysis reveals three distinct periods in the curves.

In the initial period, the atomic motion is *free*. During this period, $F_{vib}^s(q, t)$ is dominated by the leading factor in Eq. (8), $e^{-a(q)t^2}$. To estimate the duration of this period, let us average the right side of Eq. (13) over the atoms, and over the star of \mathbf{q} ; then with the eigenvector orthonormality relation

$$\sum_{Ki} w_{Ki,\lambda} w_{Ki,\lambda'} = \delta_{\lambda\lambda'} \quad (15)$$

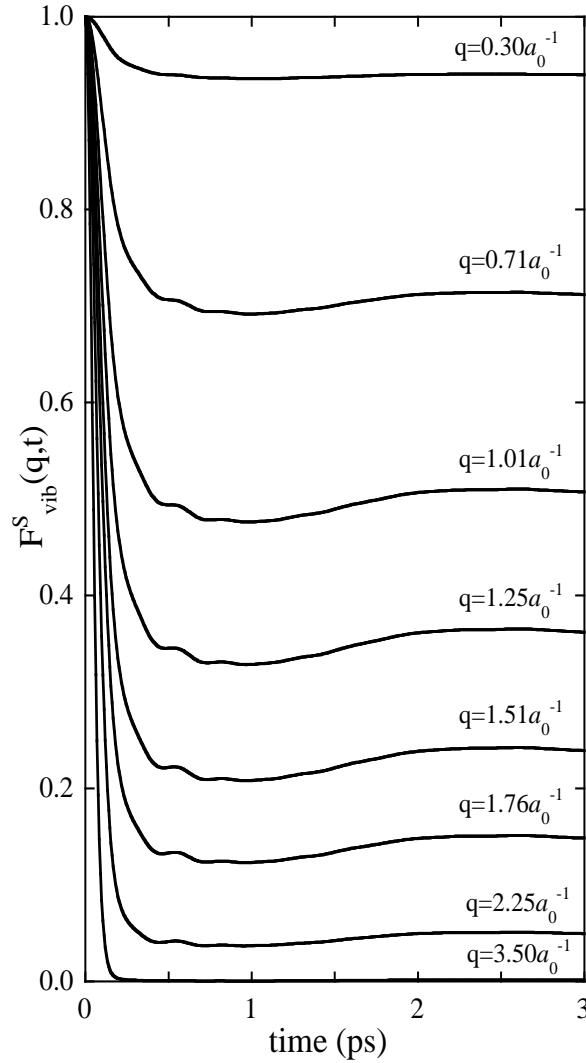


FIG. 1: $F_{vib}^s(q, t)$ for a wide range of q , showing the initial decrease on a q -independent timescale, and universal behavior where the function converges to its $t = \infty$ limit.

we find

$$\frac{1}{N} \sum_K \langle (\hat{q} \cdot \mathbf{w}_{K\lambda})^2 \rangle_{\mathbf{q}} = \frac{1}{3N}. \quad (16)$$

Accordingly

$$F_{vib}^s(q, t) \approx e^{-a(q)t^2 + b(q)t^4 - \dots}, \quad (17)$$

where

$$b(q) = \frac{kTq^2}{24M} \langle \omega_\lambda^2 \rangle, \quad (18)$$

and where $\langle \omega_\lambda^2 \rangle = (3N)^{-1} \sum_\lambda \omega_\lambda^2$. The free motion period will last until the t^4 term in Eq. (17) begins to be felt; let us therefore choose τ_f , the duration of this period, as the time when $b(q)t^4 = 0.1a(q)t^2$, giving $\tau_f = \sqrt{1.2/\langle \omega_\lambda^2 \rangle}$. Because of the decoupling approximation used in deriving Eq. (17), τ_f is independent of q . $\langle \omega_\lambda^2 \rangle$ is related to the characteristic temperature θ_2 by $\frac{5}{3} \langle (\hbar\omega_\lambda)^2 \rangle = (k\theta_2)^2$ [19]. For our liquid Na system $\theta_2 = 154.1$ K [27], and we find $\tau_f = 0.070$ ps. Our calculations show that $F_{vib}^s(q, t)$ begins to depart from $e^{-a(q)t^2}$ at a time near τ_f , specifically at around 0.08 ps at $q = 0.30 a_0^{-1}$, and decreasing to around 0.05 ps at $q = 3.50 a_0^{-1}$.

TABLE I: Infinite time limit of $F_{vib}^s(q, t)$ and decay factors $\gamma(q)$ of the transit induced decorrelation, according to Eq. (28), for different values of the wave vector q .

q (a_0^{-1})	$F_{vib}^s(q, \infty)$	$\gamma(q)$
.29711	0.94185	0.1733
.70726	0.71699	0.9222
.91575	0.57671	1.4676
1.0148	0.51138	1.7500
1.0917	0.46182	1.9753
1.1050	0.45332	2.0146
1.1443	0.42926	2.1312
1.2547	0.36482	2.4595
1.5052	0.24047	3.1805
1.7577	0.14876	3.8169
2.0041	0.08776	4.2975
2.2529	0.04903	4.6103
2.5064	0.02573	4.7423
2.8498	0.00985	4.6527
3.2000	0.00339	4.3396
3.5008	0.00126	3.9994
6.0013	0.00000	4.2271

The intermediate period in Fig. 1 follows the free period. Here the strong decrease of $F_{vib}^s(q, t)$ continues, but the function is not approximated by the $e^{-a(q)t^2}$ factor in Eq. (8). In terms of the power series expansion of the right side of Eq. (7), increasingly higher orders contribute while $F_{vib}^s(q, t)$ retains a smooth t -dependence. This property is q -independent.

At some point, the set of $\cos \omega_\lambda t$ dephase and begin to cancel, starting from the highest frequency and continuing to the lowest, which is the last to dephase. Since the highest frequency in our system is $\omega_{max} = 25.5 \text{ ps}^{-1}$ [21], the dephasing will begin around $2\pi/\omega_{max} = 0.25 \text{ ps}$. From Fig. 1, this is close to the uniform (q -independent) time when the initial decrease ends and $F_{vib}^s(q, t)$ begins to converge to its long-time limit. Hence we associate the convergence period with the normal-mode dephasing process.

The $t \rightarrow \infty$ limit is obtained by setting to zero the displacement autocorrelation functions in Eq. (4):

$$F_{vib}^s(q, \infty) = \frac{1}{N} \sum_K e^{-2W_K(q)}. \quad (19)$$

In approaching this limit, when the displacement autocorrelation functions are sufficiently small, a first-order expansion of the time dependent part is useful. With Eq. (5) this expansion reads

$$F_{vib}^s(q, t) = F_{vib}^s(q, \infty) + \frac{1}{N} \sum_K e^{-2W_K(q)} \frac{kTq^2}{M} \sum_\lambda (\hat{q} \cdot \mathbf{w}_{K\lambda})^2 \frac{\cos \omega_\lambda t}{\omega_\lambda^2}. \quad (20)$$

From Eq. (19), it is the Debye-Waller factors which set the level to which $F_{vib}^s(q, t)$ decreases in Fig. 1, and after that decrease, Eq. (20) applies. Values of $F_{vib}^s(q, \infty)$ are listed in Table I.

Fig. 1 shows a remarkable similarity of the curves in the convergence period. The main feature is a broad minimum around 1 ps, where $F_{vib}^s(q, t)$ lies below $F_{vib}^s(q, \infty)$, and a final increase of $F_{vib}^s(q, t)$ to arrive at $F_{vib}^s(q, \infty)$ by around 2 ps. These timings are accurately independent of q . Furthermore, superimposed on this broad shape is a set of small oscillatory features whose timings are also accurately independent of q . This property can be understood with the aid of a small approximation in Eq. (20). In a single random valley, the atomic sites are all inequivalent, for the same reason that different sites in a crystal unit cell are inequivalent. If we neglect the *coupling* of this inequivalence between the eigenvectors and Debye-Waller factors, we can average the $(\hat{q} \cdot \mathbf{w}_{K\lambda})^2$ as in Eq. (16) and transform Eq. (20) to

$$F_{vib}^s(q, t) \approx F_{vib}^s(q, \infty) \left[1 + \frac{kTq^2}{M} \frac{1}{3N} \sum_\lambda \frac{\cos \omega_\lambda t}{\omega_\lambda^2} \right]. \quad (21)$$

The function in brackets now exhibits uncoupled dependence on the variables kTq^2/M and t , where the t -dependence is parameterized by the set $\{\omega_\lambda\}$ of normal mode frequencies. Numerical tests verify that Eq. (21) is rather accurate in the convergence period, and this explains the uniform (q -independent) time dependence of the curves in Fig. 1.

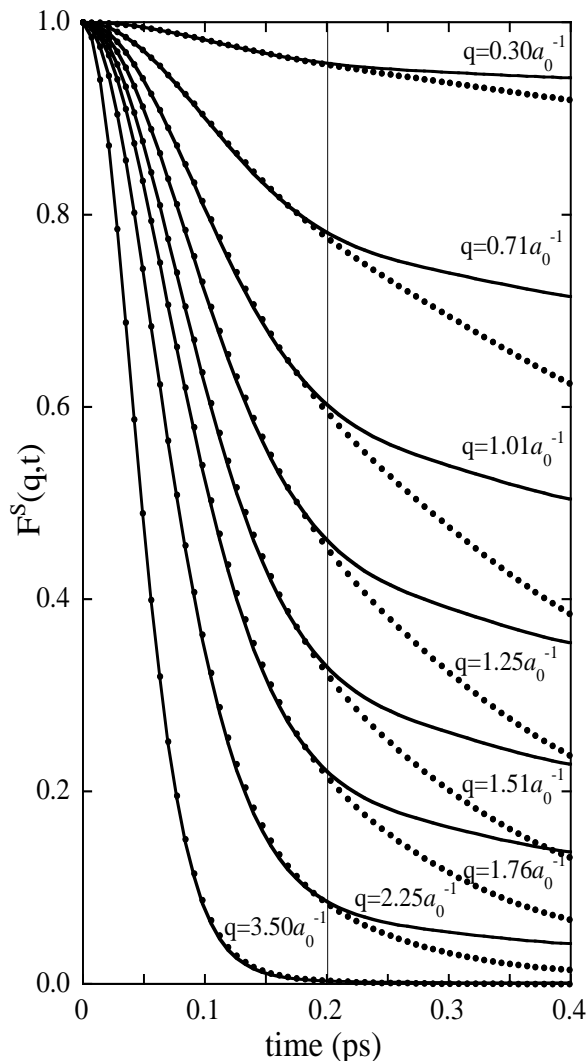


FIG. 2: For $F^s(q,t)$ the vibrational contribution (lines) and the MD data (dots) agree extremely well to around 0.2 ps (fine vertical line).

The properties of $F_{vib}^s(q,t)$ were also examined for several different random valleys in our system, and only insignificant differences were found. Hence the uniformity of random valleys previously found for equilibrium thermodynamic functions [27] is extended to the time correlation function studied here.

C. First Comparison with MD

Fig. 2 shows superimposed graphs of our MD results, $F_{MD}^s(q,t)$, and the vibrational contribution, $F_{vib}^s(q,t)$. At each q , the MD and vibrational graphs are in near perfect agreement up to an “initial departure” at around 0.2 ps. Beyond the initial departure, $F_{vib}^s(q,t)$ turns away from $F_{MD}^s(q,t)$ and proceeds to converge to its long time limit. Fig. 2 shows a remarkable constancy of the initial departure for all q , and even a remarkable constancy in the shapes of the curves in the vicinity of the departure.

Let us consider what Fig. 2 means for our analysis. $F_{vib}^s(q,t)$ is based on pure vibrational motion in a single random valley. On the other hand, $F_{MD}^s(q,t)$ is based on the real liquid motion, which has both vibrational and transit contributions. From Fig. 2, the vibrational motion completely dominates $F_{MD}^s(q,t)$ up to the initial departure. After that, the difference between $F_{MD}^s(q,t)$ and $F_{vib}^s(q,t)$ is due to transits, which are present in the MD data but not in the vibrational calculation. However, even though transits are going on continuously in the MD system, at a very high rate because the temperature is around T_m , the effect of transits does not appear immediately in $F_{MD}^s(q,t)$, but only after the motion departs from the pure vibrational motion. This observation will be used to calibrate our

decorrelation model in the next Section.

D. Transit-Induced Decorrelation

Our goal here is to model the effects of transits in a way that is consistent with the *a priori* determined vibrational motion in a single random valley. We start by returning to the definition, Eq. (1), which becomes

$$F_{VT}^s(q, t) = \frac{1}{N} \left\langle \left\langle \sum_K e^{-i\mathbf{q} \cdot (\mathbf{r}_K(t) - \mathbf{r}_K(0))} \right\rangle_{vib} \right\rangle_{trans}. \quad (22)$$

This form expresses the fundamental insight of V-T theory that the motion of the atoms consists of vibrations that are periodically modified by transits, allowing us to consider the effects of the two kinds of motion as two consecutive averages. Expanding each \mathbf{r}_K and evaluating the vibrational average as in Eqs. (2)-(4), we find

$$F_{VT}^s(q, t) = \frac{1}{N} \sum_K \left\langle e^{-i\mathbf{q} \cdot (\mathbf{R}_K(t) - \mathbf{R}_K(0))} e^{-2W_K(\mathbf{q})} e^{\langle \mathbf{q} \cdot \mathbf{u}_K(t) \mathbf{q} \cdot \mathbf{u}_K(0) \rangle_{vib}} \right\rangle_{trans}. \quad (23)$$

Notice that the equilibrium positions still carry time dependence because we have not yet evaluated the transit average. From this point of view we identify two ways in which transits will modify $F^s(q, t)$. The first arises from transit-induced changes in the atomic equilibrium positions $\mathbf{R}_K(t)$, while the second way is through their effect on the displacement autocorrelation functions $\langle \mathbf{q} \cdot \mathbf{u}_K(t) \mathbf{q} \cdot \mathbf{u}_K(0) \rangle_{vib}$. Given the fact that transits change the equilibrium positions on very short time scales compared to the vibrational motion, we expect the first effect to be largely decoupled from the second, so we make the approximation of full decoupling and find

$$F_{VT}^s(q, t) = \frac{1}{N} \sum_K \left\langle e^{-i\mathbf{q} \cdot (\mathbf{R}_K(t) - \mathbf{R}_K(0))} \right\rangle_{trans} \left\langle e^{-2W_K(\mathbf{q})} e^{\langle \mathbf{q} \cdot \mathbf{u}_K(t) \mathbf{q} \cdot \mathbf{u}_K(0) \rangle_{vib}} \right\rangle_{trans}. \quad (24)$$

Now we can consider each transit average separately.

Let us abbreviate the first transit average as $A_K(t)$. In V-T theory the motion of $\mathbf{R}_K(t)$ is entirely responsible for self diffusion, hence it is appropriately modeled as a random walk. The single atom transit rate ν is the number of transits per unit time in which a given atom is involved. Consider an increment δt sufficiently small that an atom is very unlikely to be involved in more than one transit. Then in δt , $A_K(t)$ changes by

$$\delta A_K(t) = \left\langle \left[e^{-i\mathbf{q} \cdot \mathbf{R}_K(t+\delta t)} - e^{-i\mathbf{q} \cdot \mathbf{R}_K(t)} \right] e^{i\mathbf{q} \cdot \mathbf{R}_K(0)} \right\rangle_{trans}. \quad (25)$$

In δt , each atom transits once with probability $\nu \delta t$, or else does not transit. If atom K does transit, $\mathbf{R}_K(t + \delta t) = \mathbf{R}_K(t) + \delta \mathbf{R}_K$. If atom K does not transit, $\mathbf{R}_K(t + \delta t) = \mathbf{R}_K(t)$. Eq. (25) becomes

$$\delta A_K(t) = \left\langle [e^{-i\mathbf{q} \cdot \delta \mathbf{R}_K} - 1] e^{-i\mathbf{q} \cdot (\mathbf{R}_K(t) - \mathbf{R}_K(0))} \right\rangle_{trans} \nu \delta t. \quad (26)$$

We assume $|\delta \mathbf{R}_K| = \delta R$, the same for all transits, while the direction of $\delta \mathbf{R}_K$ is uniformly distributed and uncorrelated with the other factors inside the sum. Then $[e^{-i\mathbf{q} \cdot \delta \mathbf{R}_K} - 1]$ can be separately averaged over angles and Eq. (26) can be written

$$\frac{\delta A_K(t)}{\delta t} = -\gamma(q) \left\langle e^{-i\mathbf{q} \cdot (\mathbf{R}_K(t) - \mathbf{R}_K(0))} \right\rangle_{trans} \quad (27)$$

where

$$\gamma(q) = \nu \left[1 - \frac{\sin q \delta R}{q \delta R} \right]. \quad (28)$$

Since the transit average on the right hand side of Eq. (27) is $A_K(t)$ and $A_K(0) = 1$, the equation integrates to

$$A_K(t) = e^{-\gamma(q)t}. \quad (29)$$

Finally, from this result and Eq. (4) for $F_{vib}^s(q, t)$, Eq. (24) becomes

$$F_{VT}^s(q, t) = e^{-\gamma(q)t} \langle F_{vib}^s(q, t) \rangle_{trans}. \quad (30)$$

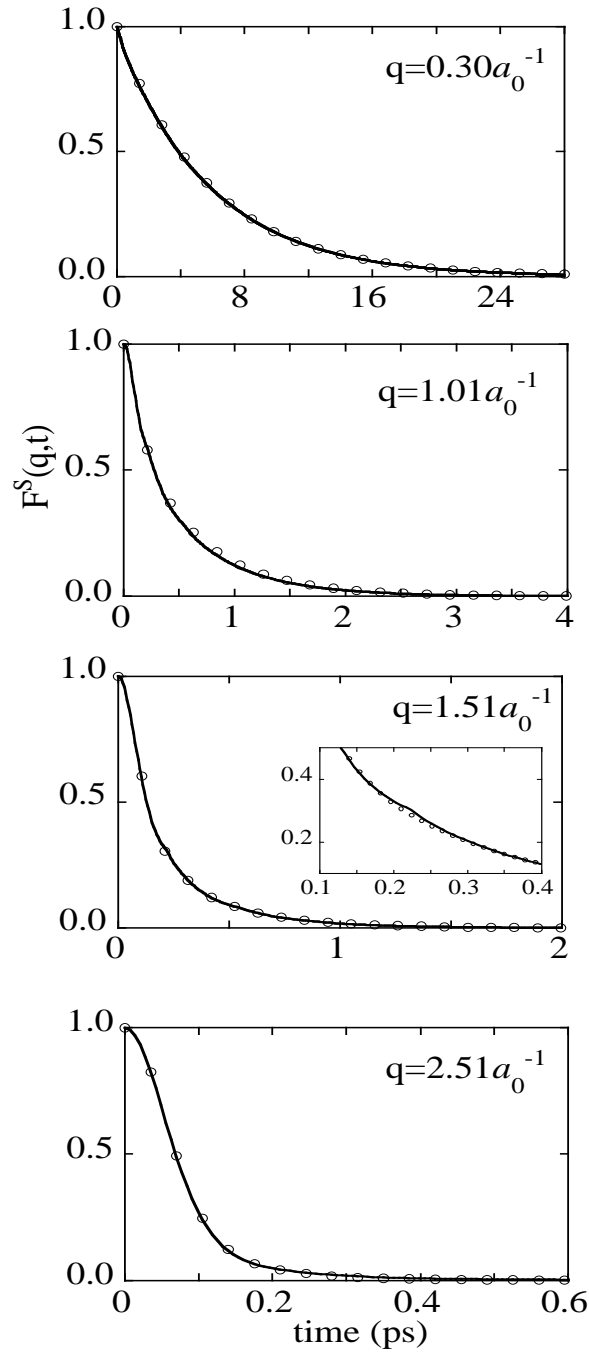


FIG. 3: Comparison of $F_{VT}^s(q, t)$ (lines) with $F_{MD}^s(q, t)$ (circles) for various q . The crossover bump near τ_c is enlarged in the graph for $q = 1.51 a_0^{-1}$.

So the random walk for $\mathbf{R}_K(t)$ in Eq. (24) yields the last relation, with the displacement autocorrelation functions in $F_{vib}^s(q, t)$ still having arbitrary time dependence.

Now we must account for the fact that the transit-induced decorrelation does not begin to operate until some time has passed (Fig. 2). We do this with the simplest possible model, replacing the decay factor $e^{-\gamma(q)t}$ by the decorrelation function $D(q, t)$, defined by

$$D(q, t) = \begin{cases} 1 & \text{for } t \leq \tau_c, \\ e^{-\gamma(q)(t-\tau_c)} & \text{for } t \geq \tau_c; \end{cases} \quad (31)$$

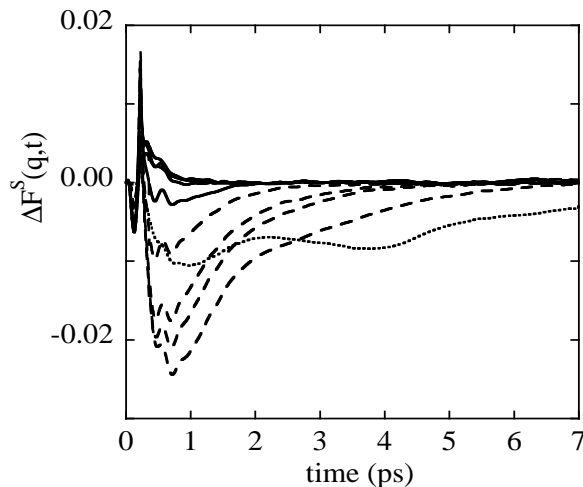


FIG. 4: Deviations of $F_{VT}^s(q, t)$ from $F_{MD}^s(q, t)$, Eq. (35). The dotted line is $q = 0.30 a_0^{-1}$, the four dashed lines are (from the lowest) $q = 0.71, 0.92, 1.01, \text{ and } 1.25 a_0^{-1}$, and the solid lines show negligible deviation for $q \geq 1.51 a_0^{-1}$.

where τ_c is the crossover time, to be calibrated. Then from Eq. (30), our transit decorrelation model is now

$$F_{VT}^s(q, t) = \langle F_{vib}^s(q, t) \rangle_{trans} D(q, t). \quad (32)$$

In the random walk model, the self diffusion coefficient is $D = \frac{1}{6}\nu(\delta R)^2$. A measurement of δR was obtained from MD simulations at 30 K [28], and the result can be used here because δR has only weak T dependence. On the other hand, ν is a strong function of T , so we use the MD evaluation $D_{MD} = 5.61(10^{-5}\text{cm}^2/\text{s})$ at the temperature of the present study, 395 K [29]. For comparison, the experimental value for liquid Na at 395 K is $5.08(10^{-5}\text{cm}^2/\text{s})$ [30]. The results for δR and ν are

$$\begin{aligned} \delta R &= 1.75 a_0, \\ \nu &= 3.9 \text{ ps}^{-1}. \end{aligned}$$

The value of ν is not far from our previous estimate of 2.5 ps^{-1} [31]. Data for $\gamma(q)$ are listed in Table I.

The second effect of transits is felt on the displacement correlation functions. As noted in Sec. IIB, these functions already decay to zero by the natural decorrelation among normal modes. As a model, we might suppose that transits cause sudden vibrational phase shifts, and therefore enhance the decay of the displacement autocorrelation functions. This enhanced decay will cause $F_{vib}^s(q, t)$ to decay more quickly to $F_{vib}^s(q, \infty)$. Referring to the curves in Fig. 1, the main effect will be to slightly raise the broad minimum around 1 ps, and bring the curve to $F_{vib}^s(q, \infty)$ noticeably before 2 ps. This is an interesting physical effect, but is small; in fact it is extremely small compared to the decorrelation caused by the motion of the equilibrium positions, as modeled in Eq. (31). We therefore neglect the transit-induced decorrelation of the displacement autocorrelation functions in the present study, with the final result that

$$F_{VT}^s(q, t) = F_{vib}^s(q, t)D(q, t). \quad (33)$$

Now the only thing that remains to be determined is the parameter τ_c . The foremost property revealed in Fig. 2 is that τ_c must be independent of q . For this reason it is conceivable that vibrational information alone can determine τ_c . We have clues to this effect – for example, τ_c is close to the start of dephasing at 0.25 ps (Sec.IIB) – but we have no certainty. We therefore calibrate τ_c by comparison of the theoretical $F_{VT}^s(q, t)$, Eq. (33), with the MD results in Fig. 2, at t around τ_c . This gives $\tau_c = 0.22$ ps. The reason τ_c is a little larger than the initial departure time of 0.20 ps in Fig. 2 is to allow the discontinuous $D(q, t)$, Eq. (31), to better fit the actual smooth crossover behavior. When τ_c is determined in the same way for different random valleys, the scatter in τ_c is around ± 0.01 ps.

E. The Hydrodynamic Limit

The hydrodynamic limit corresponds to $q \rightarrow 0$ and t larger than a characteristic time. As $q \rightarrow 0$, from Eqs. (4)-(6), $F_{vib}^s(q, t) \rightarrow 1 + O(q^2)$ for $0 \leq t \leq \infty$. Also as $q \rightarrow 0$, $\gamma(q) \rightarrow O(q^2)$, and from Eq. (31), $D(q, t) \rightarrow e^{-\gamma(q)t}[1 + O(q^2)]$

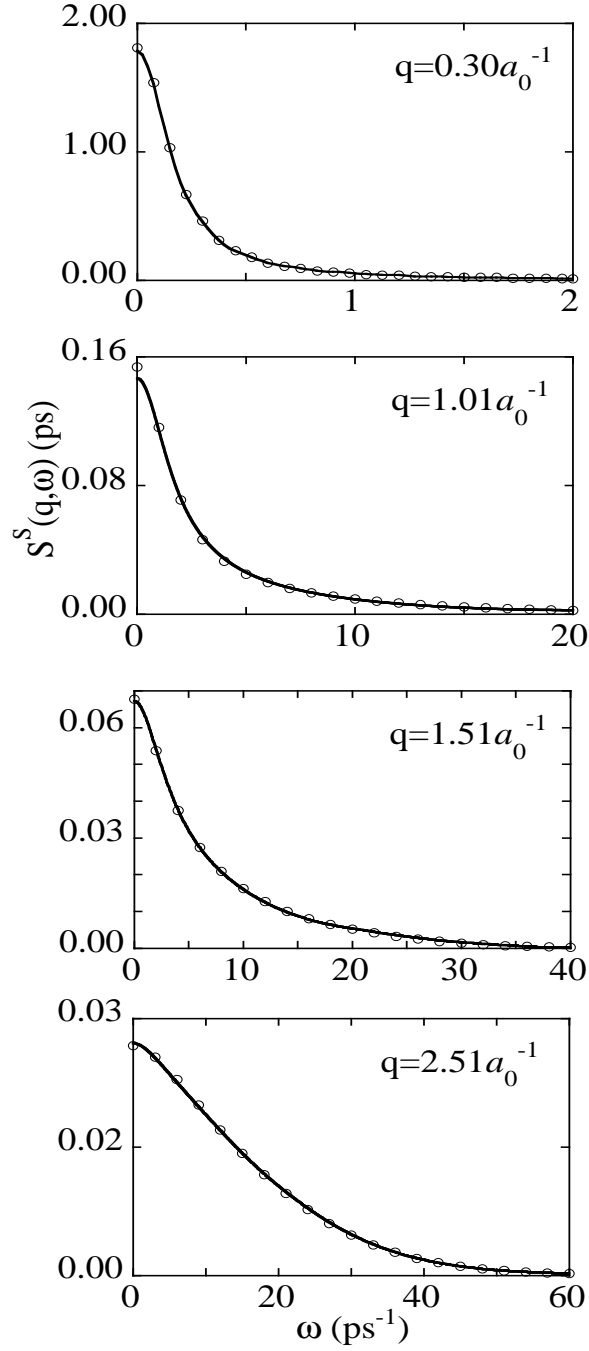


FIG. 5: Comparison of $S_{VT}^s(q, \omega)$ (lines) with $S_{MD}^s(q, \omega)$ (circles) for various q .

for $t > \tau_c$. Then from Eq. (33), $F_{VT}^s(q, t)$ is $e^{-\gamma(q)t}[1 + O(q^2)]$. We drop the term in $O(q^2)$ and take the $q \rightarrow 0$ limit of $\gamma(q)$, Eq. (28), to find

$$\lim_{q \rightarrow 0} F_{VT}^s(q, t) = e^{-Dq^2 t} \text{ for } t > \tau_c, \quad (34)$$

where we used the random walk model expression for the self diffusion coefficient. The right side is the correct hydrodynamic limit of $F^s(q, t)$.

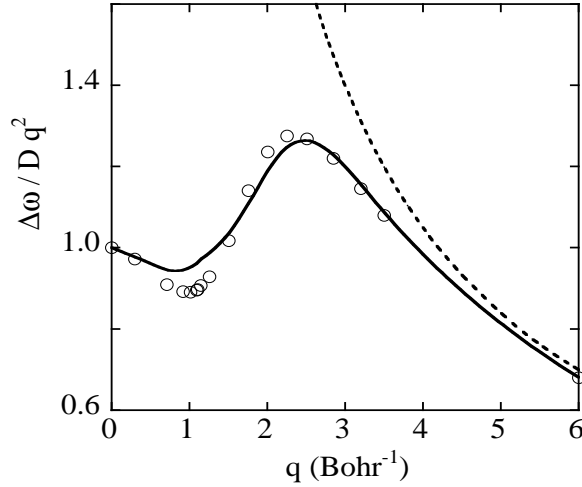


FIG. 6: Comparison of theory (solid line) and MD (circles) for the normalized halfwidth of $S^s(q, \omega)$ for all q listed in Table I. The dashed line is the free-particle limit.

III. COMPARISON OF THEORY WITH MD CALCULATIONS

A. Self Dynamic Response

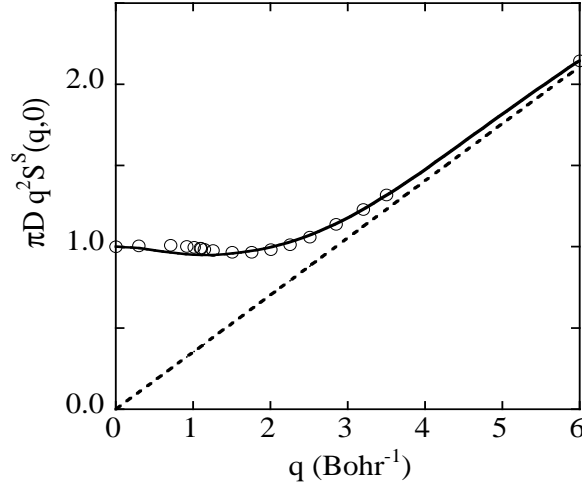


FIG. 7: Comparison of theory (solid line) and MD (circles) for the normalized value of $S^s(q, 0)$ for all q listed in Table I. The dashed line is the free-particle limit.

Graphs comparing theory with MD are shown in Fig. 3 for $q = 0.30 - 2.51 a_0^{-1}$. The time required to decay to zero decreases strongly as q increases, from around 28 ps at $q = 0.30 a_0^{-1}$ to 0.6 ps at $q = 2.51 a_0^{-1}$. The decay rates $\gamma(q)$, Table I, show a corresponding strong increase as q increases. Since the decorrelation begins at $\tau_c = 0.22$ ps, nearly the entire curve at $q = 0.30 a_0^{-1}$ is the decay process. The decorrelation steadily becomes a smaller part of the curve as q increases, until it affects only the tail of the curve at $q = 2.51 a_0^{-1}$. These changes are accompanied by a change in shape of the graphs, from a near-exponential at $q = 0.30 a_0^{-1}$, going over to a qualitatively Gaussian shape at $q = 2.51 a_0^{-1}$. All of this behavior has the important consequence that the decay rate $\gamma(q)$ eventually becomes irrelevant as q increases.

Generally speaking, the crossover bump in the theoretical curve around τ_c cannot be seen in graphs as small as those in Fig. 3. The prominence of the bump depends on both the slope and magnitude of the curve at τ_c . It is most prominent at $q = 1.51 a_0^{-1}$, where it is enlarged in the inset. The deviations

$$\Delta F^s(q, t) = F_{VT}^s(q, t) - F_{MD}^s(q, t) \quad (35)$$

for representative q are shown in Fig. 4. The largest deviations in our study are included in the figure. For most q and most t , the deviation is $\lesssim 0.005$ in magnitude, which we consider insignificant. Larger deviations are seen in two places. (a) The positive spike at $t \approx 0.22$ ps is due to the crossover model, Eq. (31). This error could be removed by smoothing, but since it is so small we are willing to forego the introduction of a smoothing model. (b) The only significant deviations are those in the negative dip at $t \sim 0.3 - 2.0$ ps. These deviations reach magnitude $\sim 0.01 - 0.02$ for the dotted curve ($q = 0.30 a_0^{-1}$) and the four dashed curves ($q = 0.71 - 1.14 a_0^{-1}$). Notice the shape at $q = 0.30 a_0^{-1}$ is the same as the others, but stretched out over a much longer time. This error arises from the broad shallow minimum in $F_{vib}^s(q, t)$ observed in Fig. 1. That minimum is not entirely in error, however, since a weakened copy of it is present in $F_{MD}^s(q, t)$. From a detailed examination of the data, we conclude that the error can be eliminated by adding a theoretical model for the transit-induced decorrelation of the displacement autocorrelation functions. This decorrelation process was discussed at the end of Sec. IID.

Graphs comparing theory with MD for $S^s(q, \omega)$ are shown in Fig. 5. The only significant error corresponds to the negative dip in $\Delta F^s(q, t)$ for a limited q range, in Fig. 4. This q range is near the location of the first peak in $S(q)$, at $q_m = 1.05 a_0^{-1}$ in our system.

Further comparison of theory and MD is shown in Figs. 6 and 7. The quantity graphed in Fig. 6 is $\Delta\omega(q)/Dq^2$, where $\Delta\omega(q)$ is the halfwidth of $S^s(q, \omega)$ and Dq^2 is the halfwidth in the diffusion limit [24, 25]. Fig. 7 shows the quantity $\pi Dq^2 S^s(q, 0)$, where $(\pi Dq^2)^{-1}$ is $S^s(q, 0)$ in the diffusion limit [22]. In these graphs we used the same value D_{MD} for Na at 395 K as in calibrating $\gamma(q)$ following Eq. (33). These figures will allow a comparison of the present theory with the traditional generalized hydrodynamics and mode coupling theories in Sec. IV. Here we observe that Figs. 6 and 7 show a rather good agreement between theory and MD for the entire q range, including the approach to the free-particle limit. Further, most of the error revealed in Figs. 6 and 7 appears in the vicinity of q_m and is attributed to our neglect of the transit-induced decorrelation of the displacement autocorrelation functions in Eq. (4).

B. Approach to the Free-Particle Limit

According to Eq. (14), $F_{vib}^s(q, t)$ reaches the free-particle limit as $q \rightarrow \infty$. When the transit-induced motion of the equilibrium positions is accounted for, the V-T theory expression is Eq. (33), with $D(q, t)$ given by Eq. (31). The approach of $F_{VT}^s(q, t)$ to the free-particle limit is therefore to be understood by watching the function $F_{vib}^s(q, t)D(q, t)$ as q increases. The process contains two steps, both operating at all times, but in effect more or less sequential, as follows.

(a) In the first step, because $F_{vib}^s(q, t)$ decreases to zero in an ever shorter time as q increases, and because $D(q, t) = 1$ for $t \leq \tau_c$, the decorrelation function effectively approaches 1 as q increases. This process is apparent in Fig. 2. Let us define q_c by the condition that $D(q, t)$ can be replaced by 1 for $q \geq q_c$. Then

$$F_{VT}^s(q, t) = F_{vib}^s(q, t), \quad \text{for } q \geq q_c. \quad (36)$$

This is the situation in Fig. 8 at $q = 3.50 a_0^{-1}$: $D(q, t)$ is effectively 1 for all time, and as a result, F_{VT}^s and F_{MD}^s are in near perfect agreement for all time.

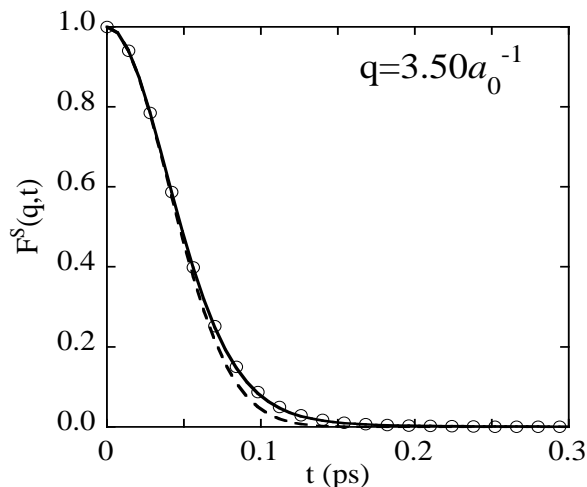


FIG. 8: $F^s(q, t)$ at $q \approx q_c$. Solid line is V-T theory, circles are MD, and dashed line is the free-particle theory, Eq. (12).

(b) In exact free-particle motion, the self intermediate scattering function is given by Eq. (12). But when step (a) is completed and Eq. (36) holds, and $F_{vib}^s(q, t)$ agrees with $F_{MD}^s(q, t)$, these functions have not yet reached the free-particle limit. This is also shown in Fig. 8, where the theory and MD curves differ noticeably from the free-particle curve. The situation exemplifies the point discussed in Sec. IIB, that in the intermediate time period, $F_{vib}^s(q, t)$ continues its steep decrease but is not well approximated by the $e^{-a(q)t^2}$ factor. So the final step in arriving at the free-particle limit is to increase q beyond q_c , until $F_{vib}^s(q, t)$ coincides with $F_{free}^s(q, t)$.

Fig. 9 shows the Fourier transform of Fig. 8. Again the theory and MD are in agreement while both differ from the free-particle curve. Another view of the approach to the free-particle limit is seen in Fig. 6. For the halfwidth, the difference between theory and MD is around 0.8% for $q = 2.51 - 3.50 a_0^{-1}$, and is 0.1% at $q = 6.00 a_0^{-1}$. This level of agreement is in strong contrast to the much larger difference of theory and MD from the free-particle halfwidth. The same property for $S^s(q, 0)$ is observed in Fig. 7. Clearly theory and MD are in substantial agreement long before they arrive at the free-particle limit. Then, the final approach to the free particle limit is determined entirely by the vibrational contribution, and is very slow, possibly algebraic, as seen in Figs. 6 and 7.

IV. SUMMARY AND CONCLUSIONS

A. Vibrational Contribution

The main conclusions of this study are expressed through a discussion of the self intermediate scattering function. We begin by comparing properties of $F_{vib}(q, t)$ with exact theory and with MD results.

(a) The short-time expansion is Eqs. (8), (10), and (13). The value at $t = 0$ is $F_{vib}^s(q, 0) = 1$, the exact result. The expansion gives the free-particle limit $F_{free}^s(q, t) = e^{-a(q)t^2}$ as the leading factor in $F_{vib}^s(q, t)$, at all q . The result is not trivial. It appears because the eigenvector completeness relation Eq. (11) decouples the free-particle motion in the exponent. This property ensures that V-T theory will automatically give the free-particle behavior as $q \rightarrow \infty$.

(b) At the end of the period of free-particle motion, at $t = \tau_f$, $F_{vib}^s(q, t)$ starts to depart from $e^{-a(q)t^2}$. $F_{vib}^s(q, t)$ continues its strong decrease throughout the intermediate period, until $F_{vib}^s(q, t)$ levels off and starts to converge to $F_{vib}^s(q, \infty)$. The power series in t^2 does not usefully represent $F_{vib}^s(q, t)$ in the intermediate period. $F_{vib}^s(q, t)$ is in very good agreement with $F_{MD}^s(q, t)$ for all times up to near the end of the intermediate period, and all q , Fig. 2. This period of agreement between $F_{vib}^s(q, t)$ and $F_{MD}^s(q, t)$ is three times longer than the duration τ_f of free-particle motion, providing direct confirmation that normal mode vibrational correlations are present in the motion of the liquid state.

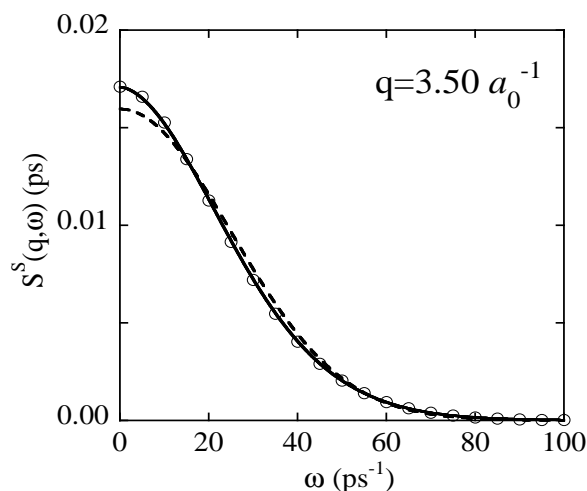


FIG. 9: $S^s(q, \omega)$ at $q \approx q_c$. Solid line is V-T theory, circles are MD, and dashed line is the free-particle theory.

B. Transit Contribution

To complete the theory for the self intermediate scattering function, we must include the transit motion. What is needed is a physically motivated model which will not interfere with the above listed accurate properties of the vibrational contribution. In Eq. (4) for $F_{vib}^s(q, t)$, there are two places where transits will cause decorrelation of the purely vibrational atomic motion.

(a) The first effect of transits is to make the equilibrium positions time-dependent in Eq. (2), i.e. $\mathbf{R}_K(t)$. This motion is modeled as a random walk of transit jumps $\delta\mathbf{R}_K$, all of the same magnitude δR , and uniformly distributed over angles for each atom. This transit motion then decouples from the vibrational motion, to give the complete theory in the form of Eqs. (31) and (33). The random walk model is calibrated *a priori* from MD data for the transit jump distance and the self diffusion coefficient. The crossover time τ_c is the only parameter calibrated with the aid of MD data for self intermediate scattering. The transit decorrelation embodied in $D(q, t)$ constitutes a major correction to $F_{vib}^s(q, t)$, and brings $F_{VT}^s(q, t)$ into excellent overall agreement with $F_{MD}^s(q, t)$.

(b) The displacement autocorrelation functions, written in Eq. (5), decay to zero as $t \rightarrow \infty$, by virtue of the natural decorrelation among normal mode vibrations. The second transit effect will be to *enhance* this decay. To make a proper model for this will require additional study, especially regarding the form of the decorrelation and the importance of the K dependence. In the meantime, the present study shows that this transit effect is small enough to neglect entirely and still have a highly accurate theory.

For the self function, the transition to free-particle behavior involves two sequential steps. First, with increasing q , $F_{vib}^s(q, t)$ goes to zero in a shorter and shorter time, until at q_c $F_{vib}^s(q, t)$ vanishes for $t \gtrsim \tau_c$. Then for $q \geq q_c$, $D(q, t)$ in Eq. (33) is effectively 1, so that $F_{VT}^s(q, t) = F_{vib}^s(q, t)$, and $F_{VT}^s(q, t)$ agrees with $F_{MD}^s(q, t)$. As q increases from q_c , theory and MD remain in agreement, and together they approach the free-particle limit. This final approach is within the vibrational contribution.

In contrast, the hydrodynamic limit depends entirely on the transit decorrelation. As $q \rightarrow 0$, $F_{VT}^s(q, t) \rightarrow e^{-\gamma(q)t}$ for $t > \tau_c$, and this produces the hydrodynamic limit in Eq. (34).

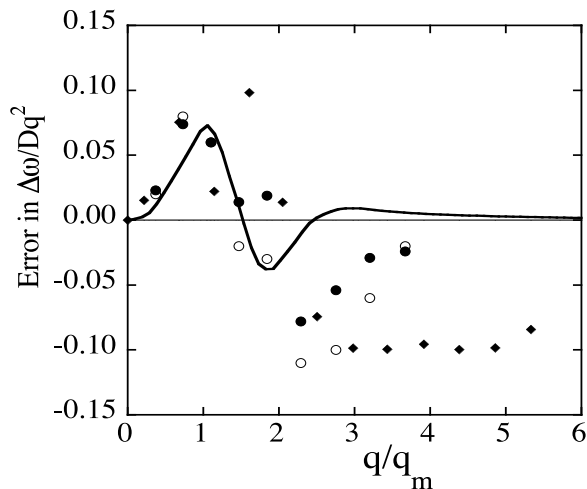


FIG. 10: Error in $\Delta\omega/Dq^2$ as function of q/q_m . Line is present theory, ($q_m = 1.05 a_0^{-1}$), open and filled circles are Ar from [22] and [23] respectively, and filled diamonds are Rb from [23].

C. Comparison with Traditional Theories

The self dynamic structure factor for liquid Ar near the triple point was studied by Levesque and Verlet [22], who compared several generalized hydrodynamics models with MD for the quantities graphed in Figs. 6 and 7. A similar study was made for liquids Ar and Rb by Wahnström and Sjögren [23], who carried out their analysis in mode coupling theory. These studies are discussed by Hansen and McDonald [24] (p. 266) and by Balucani and Zoppi [25] (Sec. 5.3), and have become the benchmark theories for $S^s(q, \omega)$. Levesque and Verlet use the memory function formalism “to give a simple phenomenological fit for the computed self intermediate scattering function.” The fitting process uses the q -dependent coefficients of t^2 , t^4 , and t^6 in $F^s(q, t)$, and is also adjusted to give the correct ideal gas (high- q) limit. Wahnström and Sjögren split the memory function into a rapid binary collision part and a slowly varying

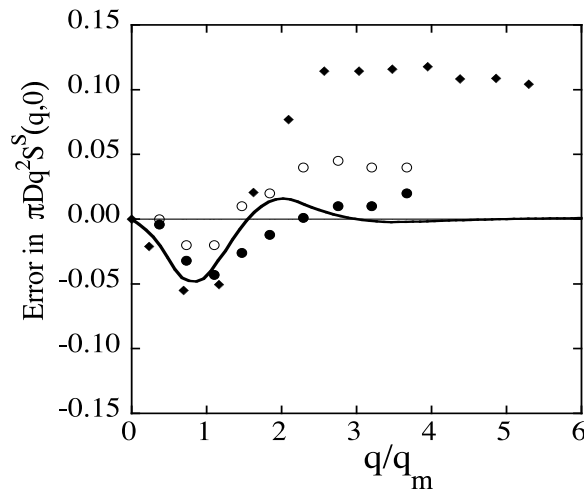


FIG. 11: Error in $\pi D q^2 S^s(q, 0)$ as function of q/q_m . Line is present theory, ($q_m = 1.05 a_0^{-1}$), open and filled circles are Ar from [22] and [23] respectively, and filled diamonds are Rb from [23].

collective recollision part. Their calibration also uses the coefficients of t^2 , t^4 , and t^6 in $F^s(q, t)$, and additional longer time information. The application of V-T theory constitutes an extreme contrast to these traditional theories. The collision concept does not appear in V-T theory. The vibrational contribution alone, *a priori* and for all q , accurately accounts for the short- and intermediate-time behavior of $F^s(q, t)$ and accurately accounts for the free-particle limit as well. Hence $F_{vib}^s(q, t)$ provides much of the information used for calibration by the traditional theories. Then, only the transit contribution remains to be addressed.

Since we are proposing a radically new theory of self dynamic response, we should compare numerical accuracy with the traditional theories. The standard for this comparison is the error of theory from MD for the quantities graphed in Figs. 6 and 7, the width and height of $S^s(q, \omega)$ [22, 23, 24, 25]. These errors, in the form of (theory-MD)/MD, are compared for traditional and present theories in Figs. 10 and 11. The Levesque and Verlet data for Ar are from their tables [22], and the Wahnström and Sjögren data for Ar and Rb are read from their graphs [23]. The large error for Rb at large q is attributed to a difference of the self diffusion coefficient between theory and MD [23]. In the overall comparison, the error in the present theory is smaller than in the traditional theories. However, in our view, more important than the comparison of numerical accuracies is the near *a priori* character of the present theory. Beyond the standard diffusional model for the motion of the vibrational equilibrium positions, only the single scalar parameter τ_c is needed to calibrate $F_{VT}^s(q, t)$ for all q and t .

APPENDIX A: OPERATIONAL PROCEDURES OF V-T THEORY

Since the operational procedures of V-T theory are somewhat novel, a brief summary will perhaps be useful. One begins with an interatomic potential for the system of interest. An MD system is constructed, and quenches are made from the liquid to minimum potential energy structures, where the equilibrium positions and the dynamical matrix are evaluated. Except for three translational eigenvalues, which are zero to numerical accuracy, all normal mode eigenvalues must be positive. In the first application to a given system, one needs to make some tests to identify the random structures (as differentiated from symmetric structures), and to verify that the random structures do indeed dominate the potential energy surface [27, 29, 32]. This step is to check the “single random valley” approximation, whose verification is still in progress [27]. From this point one can proceed by working with a single random valley. The dynamical matrix is diagonalized to find the frequencies ω_λ and eigenvectors $\mathbf{w}_{K\lambda}$. The vibrational contribution to any thermodynamic function [18, 19] or to a time correlation function [26] can be expressed in terms of these quantities. This is illustrated by the equations of Sec. II. Numerical evaluation of sums $\sum_\lambda f_\lambda$ proceeds by direct summation over the $3N - 3$ modes with nonzero ω_λ . At the present stage in the theoretical development, the transit contribution to a statistical mechanical average is accounted for by a macroscopic model, such as the one reported here in Sec. IID.

ACKNOWLEDGMENTS

Brad Clements and Renzo Vallauri are gratefully acknowledged for helpful discussions. This work was supported by the U. S. DOE under Contract No. DE-AC52-06NA25396.

-
- [1] N. W. Ashcroft and D. Stroud, in *Solid State Physics*, edited by H. Ehrenreich, F. Seitz, and D. Turnbull (Academic, New York, 1978), Vol. 33, p. 1.
 - [2] N. H. March, *Liquid Metals* (Cambridge University Press, Cambridge, 1990).
 - [3] N. W. Ashcroft, Phys. Lett. **23**, 48 (1966).
 - [4] T. E. Faber, *Theory of Liquid Metals* (Cambridge University Press, Cambridge, 1972).
 - [5] J. Hafner, in *Amorphous Solids and the Liquid State*, edited by N. H. March, R. A. Street, and M. P. Tosi (Plenum, New York, 1985), p. 91.
 - [6] W. A. Harrison, *Pseudopotentials in the Theory of Metals* (W. A. Benjamin, New York, 1966).
 - [7] A. Rahman, Phys. Rev. Lett. **32**, 52 (1974); Phys. Rev. A **9**, 1667 (1974).
 - [8] N. W. Ashcroft and D. C. Langreth, Phys. Rev. **155**, 682 (1967).
 - [9] D. C. Wallace, Phys. Rev. **176**, 832 (1968); Phys. Rev. B **1**, 3963 (1970).
 - [10] G. K. Straub, S. K. Schiferl, and D. C. Wallace, Phys. Rev. B **28**, 312 (1983).
 - [11] G. Jacucci, M. L. Klein, and R. Taylor, Solid State Comm. **19**, 657 (1976).
 - [12] U. Balucani, A. Torcini, and R. Vallauri, Phys. Rev. B **47**, 3011 (1993).
 - [13] H. R. Glyde, J. P. Hansen, and M. L. Klein, Phys. Rev. B **16**, 3476 (1977).
 - [14] G. Jacucci and I. R. McDonald, in *Liquid and Amorphous Metals*, edited by E. Lüscher and H. Coufal (Sijthoff & Noordhoff: Alphen aan den Rijn, The Netherlands, 1980), p. 143.
 - [15] N. W. Ashcroft and J. Lekner, Phys. Rev. **145**, 83 (1966).
 - [16] R. Bansal and W. Bruns, J. Chem. Phys. **80**, 872 (1984).
 - [17] P. T. Cummings and G. P. Morris, J. Phys. F: Met. Phys. **17**, 593 (1987).
 - [18] D. C. Wallace, Phys. Rev. E **56**, 4179 (1997).
 - [19] D. C. Wallace, *Statistical Physics of Crystals and Liquids* (World Scientific, New Jersey, 2002).
 - [20] D. C. Wallace, G. De Lorenzi-Venneri, and E. D. Chisolm, eprint arXiv:cond-mat/0506369.
 - [21] G. De Lorenzi-Venneri and D. C. Wallace, J. Chem. Phys. **123**, 244513 (2005).
 - [22] D. Levesque and L. Verlet, Phys. Rev. A **2**, 2514 (1970).
 - [23] G. Wahnström and L. Sjögren, J. Phys. C: Solid State Phys. **15**, 401 (1982).
 - [24] J. P. Hansen and I. R. McDonald, *Theory of Simple Liquids* (Academic, New York, 2006), 3rd ed.
 - [25] U. Balucani and M. Zoppi, *Dynamics of the Liquid State* (Clarendon Press, Oxford, 1994).
 - [26] E. D. Chisolm, G. De Lorenzi-Venneri, and D. C. Wallace, eprint arXiv:cond-mat/0702051.
 - [27] G. De Lorenzi-Venneri and D. C. Wallace, Phys. Rev. E **76**, 041203 (2007).
 - [28] D. C. Wallace, E. D. Chisolm, and B. E. Clements, Phys. Rev. E **64**, 011205 (2001).
 - [29] D. C. Wallace and B. E. Clements, Phys. Rev. E **59**, 2942 (1999).
 - [30] S. J. Larson, C. Roxbergh, and A. Lodding, Phys. Chem. Liq. **3**, 137 (1972).
 - [31] D. C. Wallace, Phys. Rev. E **58**, 538 (1998).
 - [32] B. E. Clements and D. C. Wallace, Phys. Rev. E **59**, 2955 (1999).